

Immunohistochemical Detection of Neural Stem Cells and Glioblastoma Stem Cells in the Subventricular Zone of Glioblastoma Patients

Vashendriya V.V. Hira, Remco J. Molenaar, Barbara Breznik, Tamara Lah, Eleonora Aronica, and Cornelis J.F. Van Noorden*

Department of Genetic Toxicology and Cancer Biology, National Institute of Biology, Ljubljana, Slovenia (VVVH, RJM, BB, TL, CJFVN), and Department of Medical Oncology (RJM), Department of Medical Biology (CJFVN) and Department of Neuropathology (EA), Cancer Center Amsterdam, Amsterdam UMC at the Academic Medical Center, Amsterdam, The Netherlands

Summary

Glioblastoma usually recurs after therapy consisting of surgery, radiotherapy, and chemotherapy. Recurrence is at least partly caused by glioblastoma stem cells (GSCs) that are maintained in intratumoral hypoxic peri-arteriolar microenvironments, or niches, in a slowly dividing state that renders GSCs resistant to radiotherapy and chemotherapy. Because the subventricular zone (SVZ) is a major niche for neural stem cells (NSCs) in the brain, we investigated whether GSCs are present in the SVZ at distance from the glioblastoma tumor. We characterized the SVZ of brains of seven glioblastoma patients using fluorescence immunohistochemistry and image analysis. NSCs were identified by CD133 and SOX2 but not CD9 expression, whereas GSCs were positive for all three biomarkers. NSCs were present in all seven samples and GSCs in six out of seven samples. The SVZ in all samples were hypoxic and expressed the same relevant chemokines and their receptors as GSC niches in glioblastoma tumors: stromal-derived factor-1 α (SDF-1 α), C-X-C receptor type 4 (CXCR4), osteopontin, and CD44. In conclusion, in glioblastoma patients, GSCs are present at distance from the glioblastoma tumor in the SVZ. These findings suggest that GSCs in the SVZ niche are protected against radiotherapy and chemotherapy and protected against surgical resection due to their distant localization and thus may contribute to tumor recurrence after therapy. (J Histochem Cytochem 69: 349–364, 2021)

Keywords

glioblastoma, glioblastoma stem cell, neural stem cell, niche, subventricular zone, therapy-resistance

Introduction

Glioblastoma is the most common malignant and aggressive brain tumor in adults with poor survival of approximately 20 months after diagnosis despite optimal therapy (i.e. surgical resection of the tumor, radiotherapy, temozolomide chemotherapy, and magnetic tumor-treating fields) in the fittest patient population.^{1,2}

Poor patient survival is at least partly caused by the presence of a small fraction of slowly dividing glioblastoma stem cells (GSCs) in the tumor that reside in protective microenvironments called niches. In GSC niches,

GSCs are maintained in a slowly dividing or quiescent state that contributes to their therapy-resistance.^{3–14} We have characterized GSC niches in patient-derived

Received for publication August 30, 2020; accepted January 25, 2021.

*Member of The Histochemical Society at the time of publication.

Corresponding Author:

Vashendriya V.V. Hira, Department of Genetic Toxicology and Cancer Biology, National Institute of Biology, Večna Pot 111, 1000 Ljubljana, Slovenia.

E-mail: vashendriyavhira@gmail.com

glioblastoma tissue samples and elucidated that GSC niches in glioblastoma tumors are functionally similar to hematopoietic stem cell (HSC) niches in normal human bone marrow. Both niche types are exclusively periarteriolar and hypoxic.^{4,15–18} The chemokines stromal-derived factor-1 α (SDF-1 α) and osteopontin (OPN) and their receptors C-X-C receptor type 4 (CXCR4) and CD44, respectively, are involved in homing of GSCs and HSCs in their specific niches and maintenance of their stem cell characteristics. Hypoxia in the niches induces stemness of GSCs and HSCs as the transcription factors hypoxia-inducible factor (HIF)-1 α and HIF-2 α upregulate expression of SDF-1 α , CXCR4, OPN, and CD44^{4,18–20} as well as stem cell genes such as *prominin-1* (*CD133*) and *sex-determining region Y-box 2* (*SOX2*).^{21–25}

In mouse models, GSCs do not only home in hypoxic peri-arteriolar GSC niches in the tumors but also in the subventricular zone (SVZ) of the brain, where they are protected from radiotherapy and chemotherapy.^{26–28} Clinical outcome in patients is worse when glioblastoma tumors are in contact with the SVZ compared with when this is not the case.^{29–37} Furthermore, glioblastoma recurrence in patients frequently occurs in close proximity of the SVZ.³⁸

The SVZ is the largest neurogenic niche that harbors neural stem cells (NSCs) and is located at the border of the lateral ventricles in the cerebrum where NSCs divide occasionally to generate differentiated neurons, astrocytes, and oligodendrocytes.^{28,39,40} Mouse and human SVZ has been described to consist of three layers. The first layer consists of a monolayer of ependymal cells (ECs) that contain microvilli and separates the SVZ from the ventricles.^{28,41,42} The ependymal layer is important for transport of small molecules between the cerebrospinal fluid (CSF) and neuropil and forms a barrier between CSF and the brain parenchyma.^{28,42,43} The second layer is called the hypocellular gap consisting of ependymal and astrocytic cell processes and is hypothesized to be involved in the exchange of signals to establish metabolic homeostasis and to control NSC proliferation and differentiation. The third layer is a ribbon of glial fibrillary acidic protein (GFAP)-positive astrocyte-like neural progenitor cells^{28,42–44} and CD133-positive NSCs. The next layer is the transitional zone that consists of myelinated axons and oligodendrocytes.^{28,42,43}

GSCs have been shown to home in the SVZ of the brain in mouse models where they are maintained as slowly dividing cells.^{26,27,45} Homing of GSCs in the SVZ region occurs via the SDF-1 α –CXCR4 axis. CXCR4-positive GSCs are attracted to the SVZ where levels of SDF-1 α are high. In the SVZ, GSCs are protected from radiotherapy.^{26,27,45} When CXCR4–SDF-1 α interactions

are disrupted by the use of the CXCR4 inhibitor plerixafor, GSCs are able to migrate out of the niches, differentiate, and proliferate and are sensitized to radiotherapy in mouse models.^{26,27,45} In a single-arm phase I/II clinical trial, the CXCR4 inhibitor plerixafor was tested in combination with chemotherapy and radiotherapy in 29 glioblastoma patients, which yielded a median overall survival of 21.3 months.^{46,47} A phase II clinical trial is currently recruiting patients to evaluate the efficacy of plerixafor in combination with whole-brain radiotherapy and temozolomide chemotherapy (ClinicalTrials.gov Identifier: NCT03746080). The primary endpoint is 6-month progression-free survival.

OPN in the SVZ acts as a chemokine⁴⁸ for CD44-positive NSCs^{49,50} and is involved in survival of NSCs. Thus, the OPN–CD44 axis may also play a role in homing of GSCs in the SVZ.

As far as we know, the SVZ of glioblastoma patients has not yet been investigated with respect to the presence of GSCs. Because GSC niches in glioblastoma tumors are likely to be removed by surgery, the aim of this study was to investigate whether GSCs are also hiding in the protective SVZ at distance from the tumor mass and thus escape from removal by surgery.

To address this aim of the study, a thorough characterization of the SVZ of human glioblastoma patients was performed to understand how and where GSCs are localized in the SVZ, how to distinguish NSCs from GSCs, and to determine which cell types, molecules, and tissue structures are involved in the SVZ in the maintenance of stemness of NSCs and GSCs. GSCs express stem cell markers CD133 and SOX2.^{15–17,51–55} We demonstrated in our previous study that the *CD9* gene that encodes for tetraspanin, a cell surface glycoprotein, is expressed on GSCs derived from patient biopsies, whereas CD9 expression was not found on NSCs, astrocytes, and in normal brain.⁵⁶ We aimed to test the hypothesis that the SVZ as NSC niche is morphologically similar to hypoxic peri-arteriolar GSC niches in glioblastoma and that GSCs are present in the SVZ of brains of glioblastoma patients.

Materials and Methods

Cell Cultures

Human NCH421K and NCH644 GSCs^{56,57} were a generous gift from Prof. Christel Herold-Mende (Heidelberg University, Heidelberg, Germany) and K26 GSCs were isolated and propagated from a patient-derived glioblastoma sample and were cultured as 3D tumor spheres in Neurobasal medium (Gibco Life Technologies, Carlsbad, CA, USA) containing 1% penicillin/streptomycin (Sigma, St. Louis, MO, USA),

Table 1. Details of Primary Antibodies Used for Fluorescence Immunohistochemistry.

Primary Antibody	Source	Primary Antibody Dilution in PBS + 1% BSA for Fluorescence IHC	Protein Function/Characteristics
Rabbit anti-human CD133	Abcam ^a (ab19898)	1:100	Biomarker to detect NSCs and GSCs in glioblastoma
Mouse anti-human CD9	Abcam (ab2215)	1:100	Biomarker to detect GSCs in glioblastoma
Mouse anti-human SOX2	Abcam (ab171380)	1:50	Transcription factor expressed in GSCs in glioblastoma
Mouse anti-human GFAP	Abcam (ab10062)	1:500	Intermediate filament protein expressed in astrocytes
Rabbit anti-human SDF-1 α	Abcam (ab9797)	1:200	Chemokine for CXCR4-positive (stem) cells
Rabbit anti-human CXCR4	R&D Systems ^b clone 44716 (MAb172)	1:30	G-protein-coupled receptor that interacts with ligand SDF-1 α
Rabbit anti-human OPN	Abcam (ab8448)	1:100	Chemokine for CD44-positive cells
Mouse anti-human CD44	Biorad ^c (MCA2504)	1:100	Receptor that interacts with ligand OPN
Mouse anti-human HIF-1 α	Abcam (ab8366)	1:100	Transcription factor expressed in cells in hypoxic conditions
Rabbit anti-human HIF-2 α	Abcam (ab109616)	1:100	Transcription factor expressed in cells in hypoxic conditions

Abbreviations: PBS, phosphate-buffered saline; BSA, bovine serum albumin; IHC, immunohistochemistry; GSC, glioblastoma stem cell; GFAP, glial fibrillary acidic protein; SOX2, sex-determining region Y-box 2; SDF-1 α , stromal-derived factor-1 α ; CXCR4, C-X-C receptor type 4; OPN, osteopontin; HIF, hypoxia-induced factor.

^aAbcam, Cambridge, UK.

^bR&D Systems, Minneapolis, MN, USA.

^cBiorad, Hercules, CA, USA.

1% L-glutamine (Sigma), 2% B27, 0.08% basic fibroblast growth factor (bFGF; Gibco), 0.01% epidermal growth factor (EGF; Gibco) and 0.01% heparin (Sigma) at 37C in a 5% CO₂ incubator. U87 and U373 differentiated glioblastoma cells (ATTC, Teddington, Middlesex, UK) were cultured in Dulbecco's modified Eagle's medium (DMEM) medium (Sigma) containing 1% penicillin/streptomycin, 1% L-glutamine, and 10% fetal bovine serum (Gibco) at 37C in a 5% CO₂ incubator. The U87 glioblastoma cells were authenticated as described by Torsvik et al.⁵⁸

Immunocytochemistry on Human GSCs and Differentiated Glioblastoma Cells

Human U87 glioblastoma and U373 cells were cultured on glass slides in an incubator at 37C. On each glass slide, 500,000 cells were seeded. Two days after U87 and U373 cells had been seeded on glass slides, cells were fixed in 4% paraformaldehyde (Merck, Darmstadt, Germany) for 10 min, followed by a washing step using phosphate-buffered saline (PBS; Gibco) containing 1% bovine serum albumin (BSA; Sigma-Aldrich). Cells were permeabilized and nonspecific background staining was reduced by incubating cell preparations in PBS containing 1% BSA, 10% normal goat serum (Dako Glostrup, Denmark), and 0.1%

Triton-X (Sigma-Aldrich) for 1 hr at room temperature (RT). Cells were incubated overnight at 4C with primary antibodies diluted in PBS containing 1% BSA, as indicated in Table 1.

After 5 days of culture, tumor spheres of approximately 10⁶ NCH421K, NCH644, and K26 GSCs were placed in eppendorf tubes and the entire immunostaining procedure was performed in the eppendorf tubes for the GSCs to maintain the three-dimensional (3D) structure of the tumor spheres as described before.¹⁶ GSC tumor spheres were fixed in the eppendorf tubes in 4% paraformaldehyde (Merck) for 10 min, followed by a washing step using PBS containing 1% BSA. Cells were permeabilized and nonspecific background staining was reduced by incubating cell preparations in PBS containing 1% BSA, 10% normal goat serum (Dako Glostrup, Denmark), and 0.1% Triton-X (Sigma-Aldrich) for 1 hr at RT. Cells were incubated overnight at 4C with primary antibodies diluted in PBS containing 1% BSA, as indicated in Table 1.

Alexa Fluor 488-conjugated goat anti-rabbit antibodies (Life Technologies, Carlsbad, CA, USA) and Alexa Fluor 546-conjugated goat anti-mouse antibodies (Thermo Fisher Scientific, Waltham, MA, USA) were used as secondary antibodies in a dilution of 1:200 in PBS containing 1% BSA as described before.¹⁶ Incubation lasted 1 hr at RT. Cells were

Table 2. Glioblastoma Patient Characteristics.

Patient Number	Gender	Age	Therapy	Location of the Tumor	<i>IDH1-R132H</i> Mutation
1	M	47	Radiotherapy (60 Gy)	Fronto-temporal left	Yes (secondary glioblastoma)
2	M	52	Radiotherapy (60 Gy)	Occipital right	No
3	F	71	Radiotherapy (60 Gy)	Temporal right	No
4	M	44	Radiotherapy (60 Gy) + temozolomide chemotherapy	Temporal right	No
5	M	27	Radiotherapy (60 Gy) + temozolomide chemotherapy	Frontal left	No
6	M	75	Radiotherapy (60 Gy)	Temporal left	No
7	F	60	Radiotherapy (60 Gy)	Frontal right	No

Abbreviations: M, male; F, female.

washed in PBS, followed by nuclear counterstaining using 4',6-diamidino-2-phenylindole (DAPI; Sigma-Aldrich) for 5 min at RT. Cells were washed in PBS for 5 min and coverslipped using Prolong Gold mounting medium (Life Technologies). Control incubations were performed in the absence of primary antibodies.

SVZ-invaded Glioblastoma Patient Samples

Brain tissue material was obtained from seven patients (aged 27–75 years at the time of glioblastoma diagnosis: six *IDH1*-wild type and one *IDH1*-mutated glioblastoma at autopsy at the Department of (Neuro) Pathology of Amsterdam UMC, Academic Medical Center, University of Amsterdam, The Netherlands). Informed consent was obtained for the use of brain tissue for research purposes. All procedures performed using human brain tissue were in accordance with the ethical standards of the Amsterdam University Medical Center (location AMC, reference number W14_224 # 14.17.0286), local protocols, the 1964 Helsinki declaration and its later amendments, or comparable ethical standards. Human brain tissue was fixed in 10% buffered formalin and embedded in paraffin. Histological diagnosis was confirmed following the current World Health Organization classification guidelines² by two independent neuropathologists. Sections of paraffin-embedded tissue (including the SVZ region from the site of tumor localization) were cut (5 µm thick), mounted on pre-coated glass slides (Star Frost, Waldemar Knittel, Braunschweig, Germany) and processed for immunohistochemical staining. Consent for removal of the tissue and its storage in the tumor bank for research purposes was obtained and documented in the medical charts of the patients. Patient characteristics are shown in Table 2. The seven glioblastoma samples were from patients who were treated before the advent of molecular characterization as standard practice in glioblastoma care. Therefore, the samples were not genetically fully characterized

and thus next generation sequencing data of these samples was not available.

Fluorescence Immunohistochemistry Using Human SVZ-invaded Glioblastoma Paraffin Sections

Paraffin sections (5 µm thick) of human SVZ-invaded glioblastoma were stored at RT until use. Dewaxing was performed by incubation of the sections in xylene (VWR Chemicals, Atlanta, GA, USA) for 5 min and rinsing in 100%, 96%, and 70% ethanol (Merck), respectively.

Antigen-retrieval was performed in a microwave using 100 mM citrate buffer containing 0.1% Triton-X (Sigma-Aldrich), pH 6.0, for 20 min at 98C, followed by cooling down for 20 min and a washing step in PBS.⁵⁹

Sections were encircled with a PAP pen (Dako) and incubated with PBS (Gibco) containing 10% normal goat serum (Dako) and 0.1% Triton-X for 1 hr at RT to reduce nonspecific background staining and for permeabilization of the sections. Sections were subsequently incubated overnight at 4C with primary antibodies diluted in PBS containing 1% BSA (Sigma-Aldrich), as indicated in Table 1. Sections were washed three times using PBS containing 1% BSA.

Alexa Fluor 488-conjugated goat anti-rabbit antibodies (Life Technologies) and Alexa Fluor 546-conjugated goat anti-mouse antibodies (Thermo Fisher Scientific) were used as secondary antibodies in a dilution of 1:200 in PBS containing 1% BSA for 1 hr at RT. Sections were then washed in PBS, followed by nuclear counterstaining using DAPI (Sigma-Aldrich) in PBS for 5 min at RT. Next, sections were washed in PBS for 5 min and coverslipped using Prolong Gold mounting medium (Life Technologies). Afterward, sections were sealed with nail polish and dried overnight. Control incubations were performed in the absence of primary antibodies.

Hematoxylin and Eosin (HE)

For HE staining, human SVZ-invaded glioblastoma paraffin sections (5 μ m) were dewaxed in xylene and 100% ethanol. Sections were fixed with freshly prepared Formol-Macrodex (4% formaldehyde, 7.2 mM CaCl₂, 0.12 M Dextran-70, 0.12 M NaCl, and 7.96 mM CaCO₃) for 10 min, followed by a washing step in distilled water for 5 min. Nuclei were stained with hematoxylin (Sigma-Aldrich) for 30 sec and then, sections were placed in running tap water for 5 min, after which the sections were placed in distilled water. Sections were then stained with eosin (Merck) for 20 sec, dipped five times in distilled water, 15 times in 70% ethanol, 15 times in 96% ethanol, and 10 times in 100% ethanol. Afterward, sections were rinsed three times for 5 min in xylene. The sections were covered with Pertex (Histolab, Göteneburg, Sweden). All steps were performed at RT.

Periodic Acid Schiff (PAS) Staining

PAS staining was performed by the Pathology Department at the Amsterdam UMC. Human SVZ-invaded glioblastoma paraffin sections (5 μ m) were used and the staining procedure was performed automatically using an Artisan Link Pro machine (Dako, Glostrup, Denmark) and staining kits were purchased from Agilent (Santa Clara, CA, USA).

Imaging

Fluorescence imaging as well as light microscopy for the histochemical staining was performed using an Eclipse Ti-E inverted microscope and NIS-Elements AR 4.13.04 software (Nikon Instruments, Melville, NY, USA). Fluorescence staining patterns of the SVZ-glioblastoma sections and glioblastoma cells were analyzed by three independent observers (V.V.V.H., B.B., C.J.F.V.N.). Morphology and histological characteristics of the SVZ were analyzed by two independent observers on the basis of light microscopical images (V.V.V.H., C.J.F.V.N.). Fluorescence staining of GSCs in 3D tumor spheres was imaged using a confocal microscope (Leica DFC 7000 T, Wetzlar, Germany). Staining patterns were analyzed by three independent observers (V.V.V.H., B.B., C.J.F.V.N.).

The total number of NSCs and GSCs were quantified in the seven samples using image analysis and Image J software.⁶⁰ Three images per patient sample were analyzed. NSCs were quantified by the presence of CD133 and SOX2 expression. GSCs were detected and quantified by the presence of CD133 and CD9 expression. GFAP-positive cells were also quantified in the seven SVZ samples.

Results

CD133 and SOX2 as GSC and NSC Biomarkers and CD9 as Selective GSC Biomarker

To determine which biomarkers can be used to detect GSCs in glioblastoma tissue samples, immunocytochemical analysis was performed on cell lines (Fig. 1). Monolayers of U87 and U373 differentiated glioblastoma cell lines and spheroids of NCH421K, NCH644, and K26 GSC lines were characterized in vitro using immunocytochemical analysis. Monolayers of U87 differentiated glioblastoma cells did not express the stem cell biomarkers CD133 on the surface and SOX2 in the nuclei (Fig. 1A), but expressed the astrocyte marker GFAP (Fig. 1B) and CD9 (Fig. 1C). The expression patterns of U373 were similar (data not shown). In all tested conditions described above and throughout the “Results” section, control staining in the absence of the primary antibodies was negative (Supplementary Fig. 1).

Confocal microscopy of 3D tumor spheres of NCH421K GSCs showed that stem cell biomarkers CD133 and SOX2 were expressed on the surface and in the nuclei, respectively (Fig. 1D). The astrocyte biomarker GFAP was not expressed in GSCs (Fig. 1E). GSCs expressed biomarker CD9 on the surface (Fig. 1F). The expression patterns of NCH644 GSCs and K26 GSCs were similar (data not shown).

On the basis of the immunocytochemical data, CD133 and SOX2 were used for the detection of GSCs and NSCs in the SVZ of glioblastoma tissue sections. In addition, CD9 was used to discriminate between CD9-positive GSCs and normal NSCs, as NSCs and normal brain tissue have been shown to be CD9-negative in our previous study.⁵⁶

Morphological Characteristics of the SVZ of Glioblastoma Patients

To assess the morphological characteristics of the SVZ of glioblastoma patient samples, HE (Fig. 2A) and PAS (Fig. 2B) staining was performed. Figure 2 shows representative images of the morphology found in the seven SVZ samples at distance of the tumor of glioblastoma patients.

In the lateral ventricle, the choroid plexus was present that produces the CSF. Corpora amylacea were present in the SVZ of the glioblastoma patients (Fig. 2B). The numbers of corpora amylacea structures varied between the patient samples, but were found in all seven samples. The exact nature of corpora amylacea is not known but they accumulate in the human brain during aging and in neurodegenerative disorders and likely contain non-degradable waste products.⁶¹

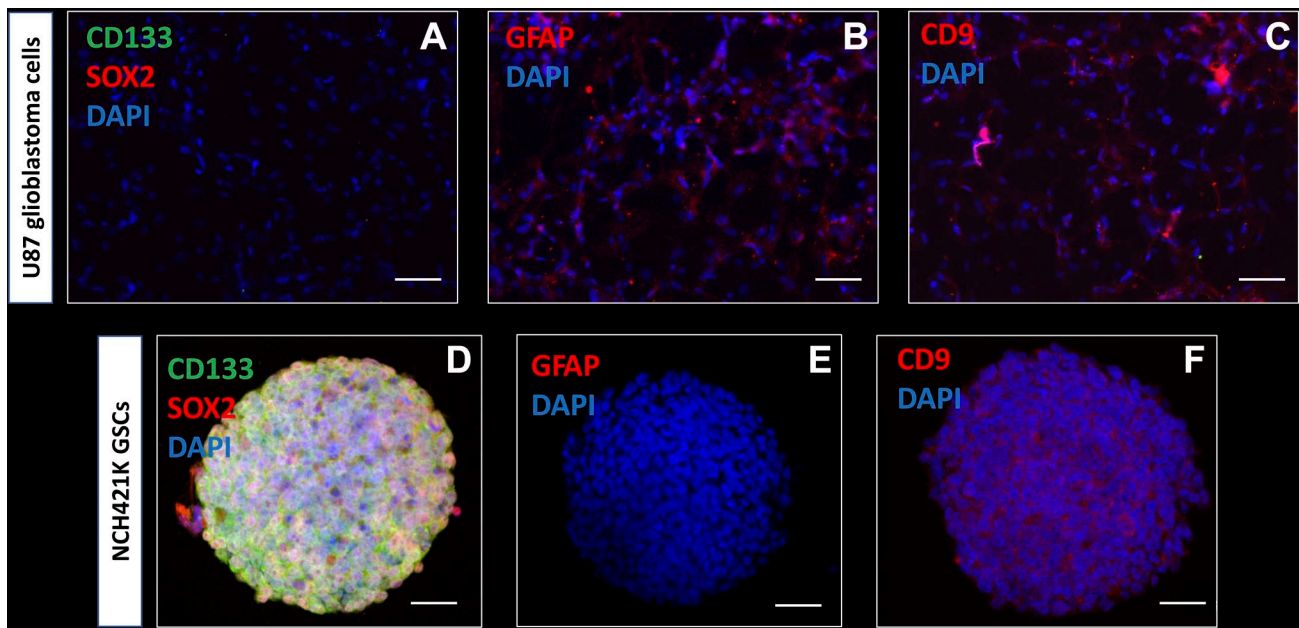


Figure 1. Immunocytochemical characterization of U87 differentiated glioblastoma cells and NCH421K GSCs. Wide-field fluorescence microscopy reveals that monolayered U87 glioblastoma cells do not express the stem cell biomarkers CD133 (green) and SOX2 (red) (A), express the astrocyte marker GFAP (B) and cell surface biomarker tetraspanin CD9 (C). Confocal microscopy demonstrates that NCH421K GSCs express the stem cell biomarkers CD133 (green) and SOX2 (red) in vitro in tumor spheres (D). GFAP is not expressed in the NCH421K GSCs in vitro in tumor spheres (E). CD9 cell surface expression is detected in NCH421K GSCs in vitro in tumor spheres (F). DAPI is used for nuclear counterstaining. Abbreviations: DAPI, 4',6-diamidino-2-phenylindole; GFAP, glial fibrillary acidic protein; GSC, glioblastoma stem cell; SOX2, sex-determining region Y-box 2. Scale bar A–C = 100 μm ; scale bar D–F = 50 μm .

The SVZ was found to be characterized by a monolayer of ECs (Fig. 2A–C) that separates the SVZ from the ventricles (Fig. 2C). GFAP staining showed the EC and astrocytic processes in the hypocellular gap (second layer) and the astrocytic-like neural progenitor cells and astrocytes in the third layer of the SVZ (Fig. 2C). All seven SVZs showed a similar morphological pattern. However, the width of the hypocellular gap varied among patient samples.

NSCs in the SVZ Express CD133 and SOX2

In the seven samples, NSCs were detected in the SVZ. NSCs expressed biomarker CD133 in the cytoplasm and on the plasma membrane (Fig. 3A) and approximately half of the CD133-positive NSCs co-expressed transcription factor SOX2 in the nuclei (Fig. 3B; Table 3). Both CD133 and SOX2 were also found to be highly expressed in the EC layer of the SVZ (Fig. 3). The ECs showed differences in cellular morphology that are most likely related to their activity. In Fig. 3A, the ECs are columnar and highly active whereas in Fig. 3B, the ECs are cuboid and more quiescent.⁶²

NSCs and GSCs Can Be Distinguished in the SVZ

Next, we determined whether GSCs were present in the SVZ samples of glioblastoma patients. GSCs were

detected using the biomarkers CD133, SOX2, and CD9, as GSCs expressed all three biomarkers in vitro (Fig. 1D and F). In the SVZ samples, NSCs did not express the biomarker CD9 (Fig. 4A), whereas GSCs expressed CD133 and CD9 on the plasma membrane (Fig. 4B and C). Thus, with the use of CD133 and CD9, NSCs and GSCs were distinguished in patient tissue samples. NSCs were found in all seven samples and GSCs were found in six out of seven patient samples. The number of NSCs and GSCs were quantified using image analysis (Table 3). The data show that the number of GSCs and NSCs varied among the patient samples. CD9 and SOX2 expression was always found in combination with CD133 expression. In addition, CD133 and SOX2 were abundantly expressed in the EC layer, whereas CD9 expression was found in the EC layer of only 1 patient sample. The number of GFAP-positive cells varied among the samples and was never found to be expressed in the EC layer.

Chemokines and Their Receptors in the SVZ

Expression of chemokines and their receptors was determined in the SVZ. The chemokine SDF-1 α was found to be highly expressed extracellularly as well as intracellularly (Fig. 5A and B). In addition, SDF-1 α was also expressed intracellularly in ECs (Fig. 5C). The receptor CXCR4 was found to be expressed on the cell

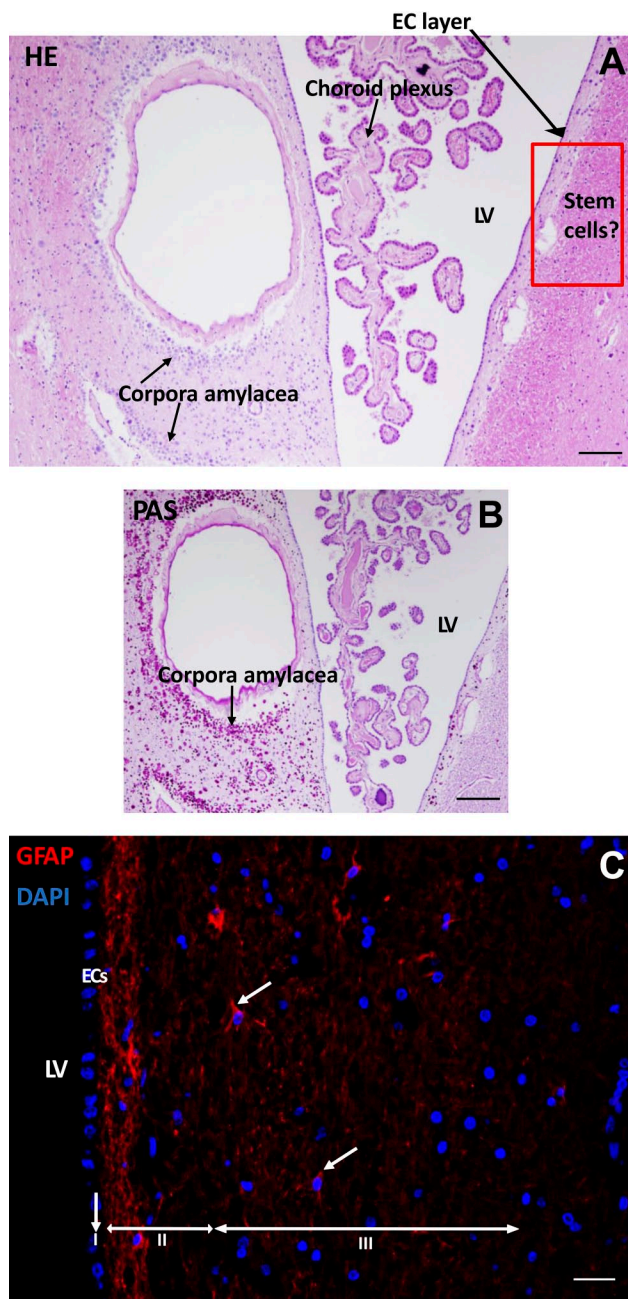


Figure 2. Morphological characteristics of the SVZ of a glioblastoma patient. HE staining shows the LV with choroid plexus inside the ventricle where CSF is produced with an EC layer lining the LV. Along the LV, corpora amylacea structures are found. The red rectangled area indicates the possible location of NSCs and GSCs (A). PAS staining demonstrates the corpora amylacea structures in the SVZ (B). Immunofluorescence staining of GFAP shows the presence of neural progenitor cells in the SVZ in red (white arrows). The three top layers of the SVZ are indicated: the monolayer of ECs (layer I), the hypocellular gap that contains EC and astrocyte processes (layer II), and the layer of NSCs and astrocytic-like neural progenitor cells that express GFAP (layer III). DAPI is used for nuclear counterstaining (C). Scale bars A, B = 100 μ m, scale bar C = 50 μ m. Abbreviations: DAPI, 4',6-diamidino-2-phenylindole; EC, ependymal cell; HE, hematoxylin and eosin; LV, lateral ventricle; CSF, cerebrospinal fluid; GFAP, glial fibrillary acidic protein; NSC, neural stem cell; PAS, periodic acid-Schiff; SVZ, subventricular zone.

surface and/or nuclei of many cell types in the SVZ, including ECs in an active state (Fig. 5A) and in a quiescent state (Fig. 5B).

We also investigated the expression of chemokine OPN, which was highly expressed intracellularly (Fig. 6A) and extracellularly (Fig. 6B) in the patient samples. Receptor CD44 was expressed on a subset of cells in the SVZ and also on ECs (Fig. 6). These expression patterns were found in all samples investigated.

The SVZ Is Hypoxic

The SVZ is hypoxic because the transcription factors HIF-1 α and HIF-2 α were present in the cytoplasm and in nuclei of cells including ECs in all seven SVZ samples. HIF-1 α was more abundantly expressed than HIF-2 α (Fig. 7). Remarkably, walls of blood vessels were strongly positive for HIF-1 α , whereas HIF-2 α expression was virtually absent in blood vessels walls (Fig. 7).

Discussion

We have immunohistochemically characterized the SVZ of glioblastoma patients to show whether the SVZ as NSC niche is morphologically similar to hypoxic peri-arteriolar GSC niches in glioblastoma and whether GSCs are present in the SVZ of brains of glioblastoma patients. To the best of our knowledge, this study is the first to demonstrate that both NSCs and GSCs are localized specifically in the human SVZ at distance of the glioblastoma tumor. Discrimination between NSCs and GSCs was performed on the basis of expression of the biomarker CD9. Furthermore, hypoxia was found to be an essential element of the SVZ, whereas the chemokines SDF-1 α and OPN and their receptors CXCR4 and CD44, respectively, were abundantly expressed in the SVZ. In Fig. 8, a schematic illustration demonstrates the morphological similarities and differences between the peri-arteriolar GSC niche in glioblastoma (Fig. 8A)^{15–18} and the SVZ as NSC niche in glioblastoma patients (Fig. 8B). Similarities between peri-arteriolar GSC niches in glioblastoma tumors and NSC niches in the SVZ are the hypoxia and the same chemokines and their receptors. The major difference is that the central role of arterioles in GSC niches is missing in the SVZ. In the SVZ, ECs and GFAP-positive cells are relevant elements of the SVZ (Fig. 8).

SVZ studies have been performed thus far almost exclusively in mouse models^{26,63–68} to elucidate the identity of NSCs. Initially, it was assumed that the monolayer of ECs of the SVZ are NSCs.^{43,69} But then, it became generally accepted that GFAP-positive cells in the SVZ are NSCs, as elimination of GFAP-positive cells resulted in loss of neurosphere-forming cells in mice.^{41,70} However, a few studies reported that GFAP-positive cells are neural progenitor cells,^{43,71} whereas

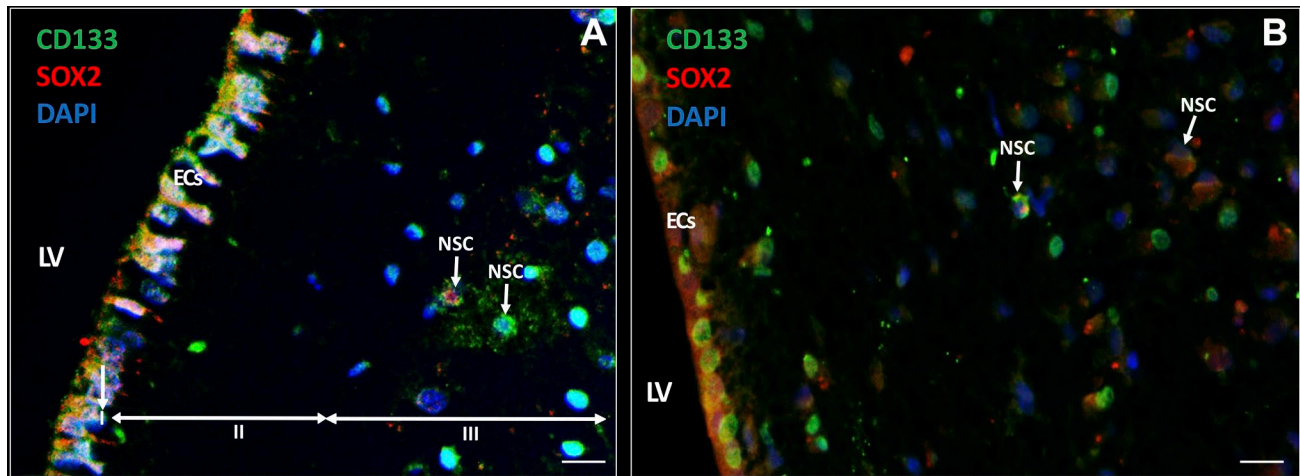


Figure 3. Immunofluorescence staining of NSCs in the SVZ of glioblastoma patients. NSCs (white arrows) express CD133 (green) and approximately half of the CD133-positive NSCs co-express SOX2 (red) in the SVZ. ECs also express CD133 and SOX2 (A, B). The ECs in (A) show characteristics of cellular activity, whereas the ECs in (B) are more quiescent. The three top layers of the SVZ are indicated: the monolayer of ECs (layer I), the hypocellular gap that contains EC and astrocyte processes (layer II), and the layer of NSCs and astrocyte-like neural progenitor cells (layer III). DAPI is used for nuclear counterstaining. Scale bar = 100 μ m. Abbreviations: DAPI, 4',6-diamidino-2-phenylindole; EC, ependymal cell; LV, lateral ventricle; NSC, neural stem cell; SOX2, sex-determining region Y-box 2; SVZ, subventricular zone.

Table 3. Numbers of GSCs and NSCs in the SVZ at Distance of the Tumor of Glioblastoma Patients.

Sample	Number of NSCs and GSCs Quantified in SVZ-Glioblastoma Samples					
	CD133 Only	CD9 Only	CD133 + CD9	SOX2 Only	CD133 + SOX2	GFAP Only
1	133 and 54 in EC layer	0	25	NA	NA	NA
2	56 and 51 in EC layer	0	33	NA	NA	18, not in EC layer
3	14 and 51 in EC layer	0	0	0	14 and 49 in EC layer	21, not in EC layer
4	24 and 26 in EC layer	0	30	NA	NA	NA
5	125 and 36 EC layer	0	79	0	125 and 48 in EC layer	10, not in EC layer
6	64 and 23 in EC layer	0	46 and 21 in EC layer	0	64 and 47 in EC layer	7, not in EC layer
7	15 and 42 in EC layer	0	41	0	15 and EC layer is damaged	24, not in EC layer
Mean	62 \pm 50	0	36 \pm 24	0	55 \pm 52	16 \pm 7

Abbreviations: EC, ependymal cell; GSC, glioblastoma stem cell; GFAP, glial fibrillary acidic protein; NSC, neural stem cell; SOX2, sex-determining region Y-box 2; SVZ, subventricular zone; NA, data not available.

NSCs express CD133 and SOX2 and can generate neurospheres that are multipotent.^{43,63,64}

On the basis of our data in human SVZ, we conclude that the CD133-positive SOX2-positive but CD9-negative cells in the third layer of the SVZ are NSCs (Fig. 4A, B) and that CD133-positive SOX2-positive CD9-positive cells in the SVZ are GSCs (Fig. 4C, D). Because GFAP is not a stem cell biomarker but a biomarker of differentiated astrocytes,^{43,66} we conclude that the GFAP-positive cells in the SVZ are astrocytes and possibly astrocytic-like neural progenitor cells.

NSCs can differentiate into neurons, astrocytes, and oligodendrocytes⁷¹ and these cell types are part of the microenvironment that is essential for the maintenance

of stemness of NSCs.⁷² In line with the above, our *in vitro* immunocytochemical analyses revealed that differentiated glioblastoma cells express GFAP (Fig. 1B) and do not express stem cell biomarkers CD133 and SOX2 (Fig. 1A), whereas GSCs do not express GFAP (Fig. 1E), but express CD133, SOX2, and CD9 (Fig. 1D, F). We also demonstrated that GSCs express receptors CXCR4 and CD44^{16,17} which are stem cell biomarkers too^{73,74} although not very specific, because these receptors are expressed by various other cell types as well (Figs. 5, 6). Heterogeneity is a hallmark of glioblastoma tumors in which various subtypes of GSCs are present.⁷⁵ GSCs that express biomarker CD44 belong to the mesenchymal subtype of GSCs and are therefore

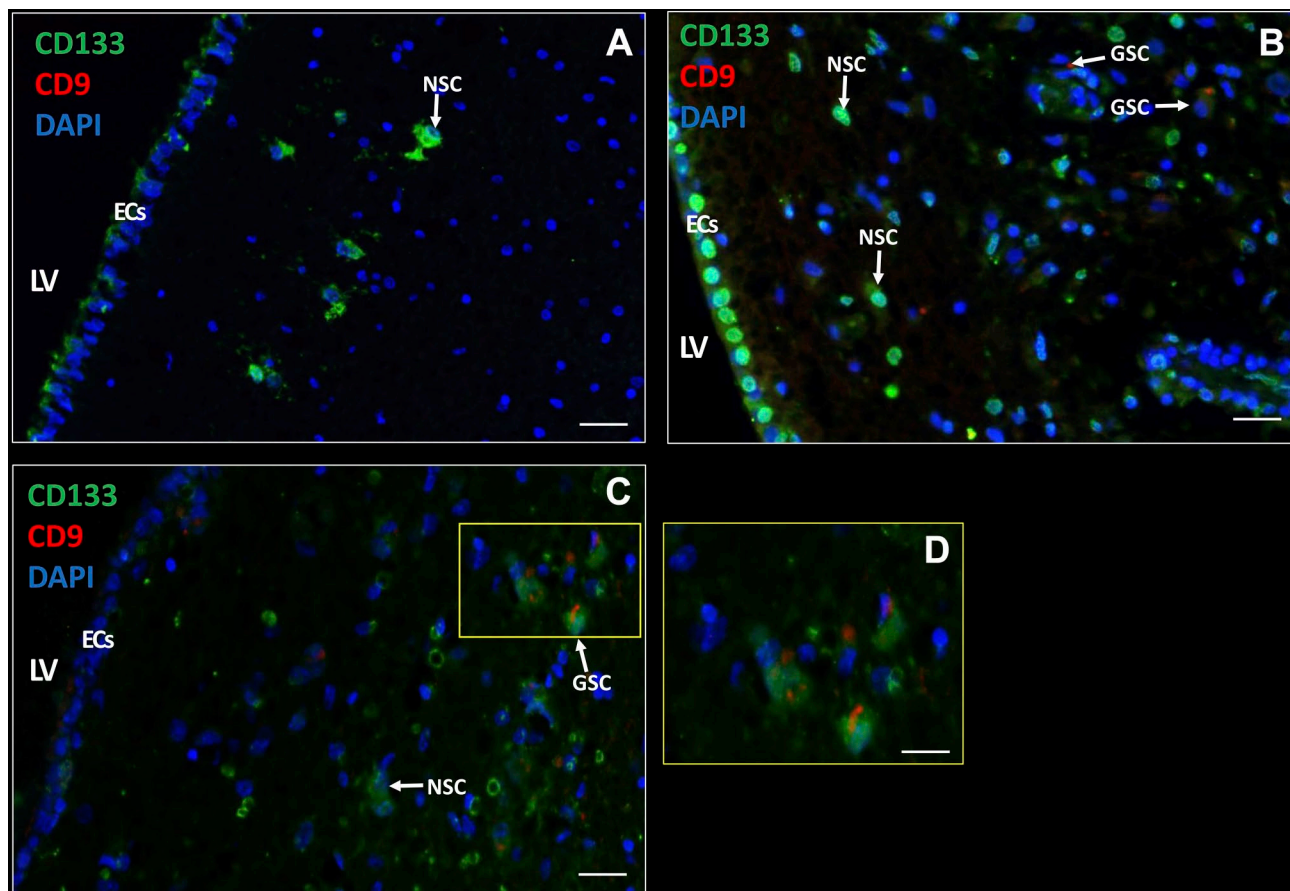


Figure 4. Immunofluorescence staining of NSCs and GSCs in the SVZ of glioblastoma patients. CD133 and CD9 expression in the SVZ of glioblastoma patients (A–D) with active ECs (A, C) and quiescent ECs (B) with variable CD133 expression (medium in A, high in B, and low in C). NSCs are characterized by CD133-positive CD9-negative and GSCs by CD133-positive CD9-positive. D is a magnification of section in C indicated by a yellow rectangle. DAPI is used for nuclear counterstaining. Scale bars: A–C = 100 μ m; D = 50 μ m. Abbreviations: DAPI, 4',6-diamidino-2-phenylindole; EC, ependymal cell; LV, lateral ventricle; NSC, neural stem cell. SVZ, subventricular zone.

most aggressive and therapy-resistant^{76,77} and their presence in the SVZ (Fig. 6) may well promote GSC survival and therapy-resistance.

The exact functions of ECs in the SVZ are still unclear. As stated above, ECs have been considered to be NSCs^{43,69} and our immunofluorescence images demonstrate that ECs express CD133 and SOX2 (Figs. 3, 4) which would be in line with their stemness. However, ECs also express chemokines SDF-1 α and OPN (Figs. 5, 6) and this expression pattern resembles that of endothelial cells which are the center of peri-arteriolar GSC niches in glioblastoma tumors. These endothelial cells also express CD133^{78–80} and SOX2 and secrete chemokines such as SDF-1 α and OPN for the maintenance of GSC stemness.^{16–18} We suggest that the ECs in the SVZ are required for the maintenance of NSCs in a similar way as endothelial cells are in peri-arteriolar GSC niches in glioblastoma. Endothelial cells have been shown to secrete factors

that are essential for the maintenance of GSC stemness.^{14,81}

Lee et al.⁸² provided evidence that glioblastoma tumors originate from SVZ-residing NSCs. It was shown in patient-derived brain tissues that NSCs in the SVZ contain driver mutations that are also present in the matching tumors at a distance from the SVZ. Moreover, NSCs that carry driver mutations migrate out of the SVZ to develop into a malignant tumor at distance in the brain.^{82,83}

The question arises whether GSCs in the SVZ are mutated NSCs^{82,83} or that they have migrated from the glioblastoma tumor into the SVZ on the basis of chemokines SDF-1 α , OPN, and/or pleiotrophin that is highly expressed by neural progenitor cells in the SVZ as was demonstrated recently in mouse models.⁶⁸

In conclusion, the SVZ as NSC niche is morphologically different from peri-arteriolar GSC niches in glioblastoma tumors but the hypoxic conditions and

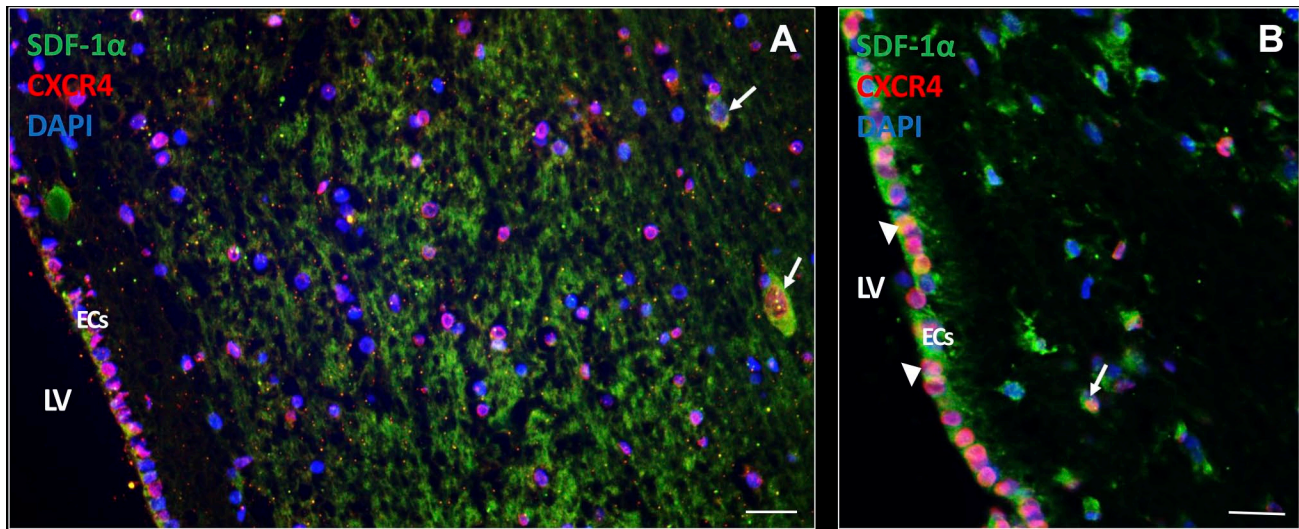


Figure 5. SDF-1 α and CXCR4 expression in the SVZ of glioblastoma patients. In the SVZ of glioblastoma patient samples, expression of the chemokine SDF-1 α is found abundantly expressed both extracellularly and intracellularly (white arrows). CXCR4 expression is present in various cell types in the SVZ, both in the cytoplasm and nucleus CXCR4 expression (A, B). SDF-1 α and CXCR4 protein expression is also found in ECs of the SVZ both in an active state (A) and a more quiescent state (white arrow heads) (B). DAPI is used for nuclear counterstaining. Scale bar A, B = 100 μ m. Scale bar C = 200 μ m. Abbreviations: CXCR4, C-X-C receptor type 4; EC, ependymal cell; DAPI, 4',6-diamidino-2-phenylindole; LV, lateral ventricle; SDF-1 α , stromal-derived factor-1 α ; SVZ, subventricular zone.

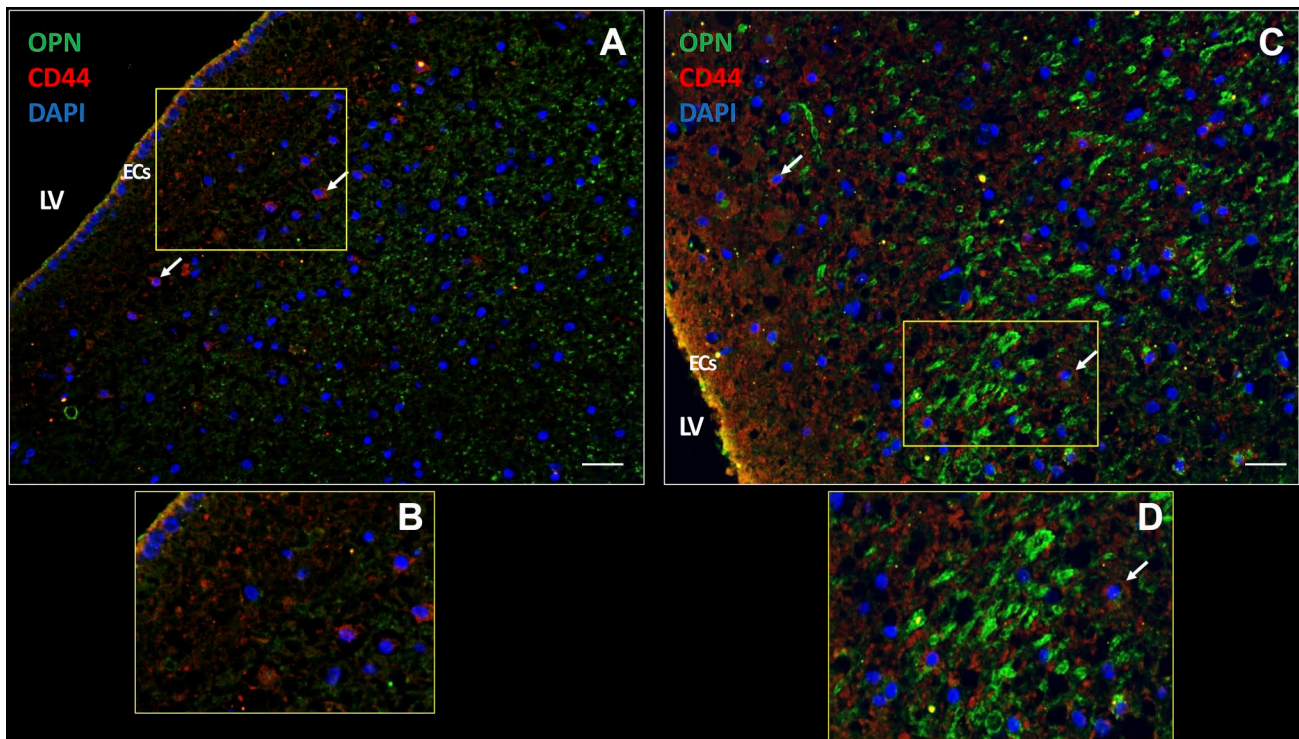


Figure 6. OPN and CD44 expression in the SVZ of a glioblastoma patient. In the SVZ, chemokine OPN is expressed extracellularly (A) as well as intracellularly (yellow dots) (C). CD44 receptor expression is present on the plasma membrane of cells in the SVZ (white arrows) (A, C). OPN and CD44 are expressed in ECs of the SVZ (yellow; C, D). B and D are magnifications of sections in A and C, respectively. DAPI is used for nuclear counterstaining. Scale bars: A = 100 μ m; B = 200 μ m. Abbreviations: DAPI, 4',6-diamidino-2-phenylindole; EC, ependymal cell; LV, lateral ventricle; OPN, osteopontin; SVZ, subventricular zone.

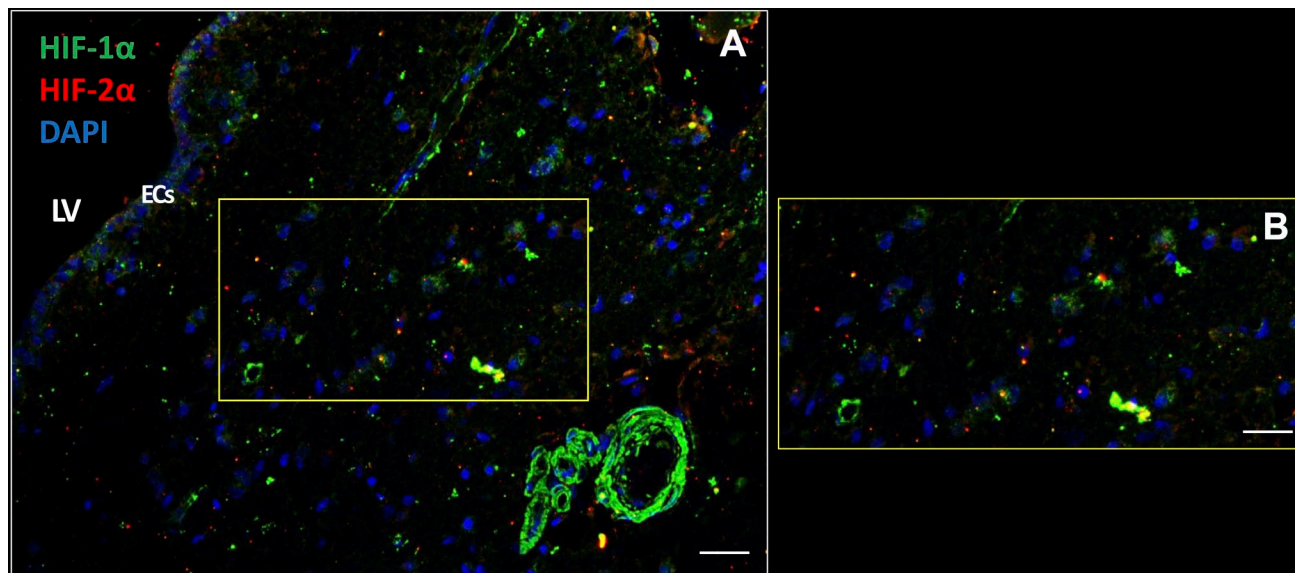
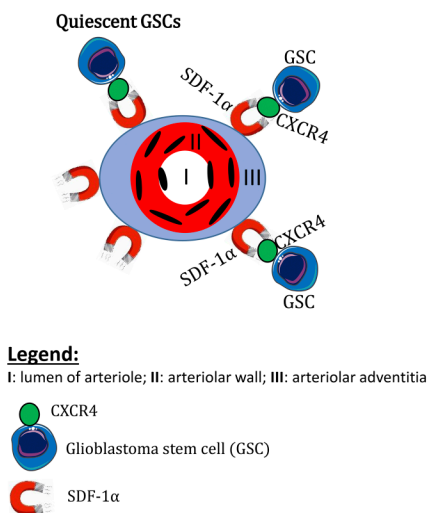


Figure 7. The SVZ niche is hypoxic. Transcription factors HIF-1 α and HIF-2 α are expressed intracellularly in the cytoplasm and nuclei of various types of cells in the SVZ of glioblastoma patient samples (A, B) including the ECs (A). HIF-1 α expression is also strongly expressed in blood vessel walls (A). DAPI is used for nuclear counterstaining. Scale bars: A = 100 μ m; B = 200 μ m. Abbreviations: DAPI, 4',6-diamidino-2-phenylindole; EC, ependymal cell; LV, lateral ventricle; HIF, hypoxia-inducible factor; SVZ, subventricular zone.

Peri-arteriolar GSC niche in glioblastoma tumor



A Subventricular zone as NSC niche in glioblastoma patients

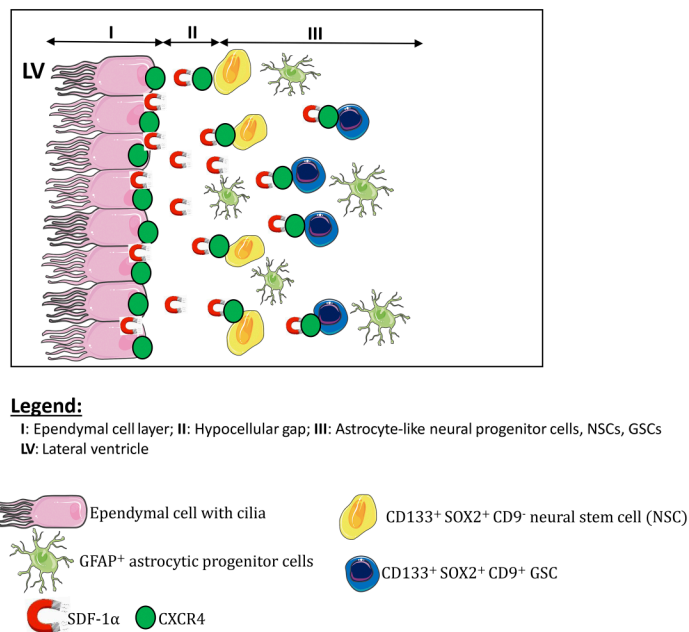


Figure 8. Schematic illustrations of niches. The peri-arteriolar GSC niche in glioblastoma tumors (A) and the SVZ as NSC niche in glioblastoma patients, containing NSCs and GSCs (B). Abbreviations: GSC, glioblastoma stem cell; NSC, neural stem cell; SVZ, subventricular zone.

presence of the same chemokines and their receptors in the SVZ indicate that the mechanisms involved in the protective conditions are similar in GSC niches and the SVZ. The presence of GSCs in the SVZ, that may well be the cause of recurrence of glioblastoma tumors after therapy, emphasizes the necessity to develop novel therapeutic treatment strategies with the aim to mobilize GSCs out of their protective perivascular GSC niches in the tumor and out of the SVZ to sensitize GSCs to chemotherapy and radiotherapy.

Acknowledgments

The authors thank Jasper Anink and Theo Dirksen from the Department of (Neuro)Pathology of the Amsterdam UMC at the location Academic Medical Center in The Netherlands for their technical assistance.

Competing Interests

The author(s) declared no potential conflicts of interest with respect to the research, authorship, and/or publication of this article.

Author Contributions

All authors have contributed to this article as follows: conception and design (VVVH, CJFVN), collection and/or assembly of data (VVVH, BB, CJFVN), data analysis and interpretation (VVVH, BB, EA, TL, RJM, CJFVN), manuscript writing (VVVH, CJFVN), final approval of manuscript (VVVH, BB, EA, TL, RJM, CJFVN), provision of study material (EA), and supervision of the entire study (CJFVN).

Funding

The author(s) disclosed receipt of the following financial support for the research, authorship, and/or publication of this article: This study was financially supported by the Dutch Cancer Society (KWF; UVA 2014-6839 and UVA 2016.1-10460; V.V.V.H., R.J.M., C.J.F.V.N.), the Slovenian Research Agency (Project J3-2526; CJFVN, BB, TL), the European Program of Cross-Border Cooperation for Slovenia-Italy Interreg TRANS-GLIOMA (Program 2017; T.L.), the IVY Interreg Fellowship (V.V.V.H.), and the Slovenian Research Agency (Program P10245; T.L., and Postdoctoral project Z3-1870 to B.B.), and R.J.M. was supported by the Fondation pour la Recherche Nuovo-Soldati 2019.

Literature Cited

1. Stupp R, Taillibert S, Kanner A, Read W, Steinberg D, Lhermitte B, Toms S, Idubai A, Ahluwalia MS, Fink K, Di Meo F, Lieberman F, Zhu J-J, Stragliotto G, Tran D, Brem S, Hottinger A, Kirson ED, Lavy-Shahaf G. Effect of tumor-treating fields plus maintenance temozolomide vs maintenance temozolomide alone on survival in patients with glioblastoma: a randomized clinical trial. *JAMA*. 2017;318(23):2306–16. doi:10.1001/jama.2017.18718.
2. Louis DN, Perry A, Reifenberger G, von Deimling A, Figarella-Branger D, Cavenee WK, Ohgaki H, Wiestler OD, Kleihues P, Ellison DW. The 2016 World Health Organization classification of tumors of the central nervous system: a summary. *Acta Neuropathol*. 2016;131(6):803–20. doi:10.1007/s00401-016-1545-1.
3. Breznik B, Limback C, Porcnik A, Blejec A, Krajnc MK, Bosnjak R, Kos J, van Noorden CJF, Lah TT. Localization patterns of cathepsins K and X and their predictive value in glioblastoma. *Radiol Oncol*. 2018;52(4):433–42. doi:10.2478/raon-2018-0040.
4. Aderetti DA, Hira VVV, Molenaar RJ, van Noorden CJF. The hypoxic perivascular glioma stem cell niche, an integrated concept of five types of niches in human glioblastoma. *Biochim Biophys Acta Rev Cancer*. 2018;1869(2):346–54. doi:10.1016/j.bbcan.2018.04.008.
5. Brooks MD, Sengupta R, Snyder SC, Rubin JB. Hitting them where they live: targeting the glioblastoma perivascular stem cell niche. *Curr Pathobiol Rep*. 2013;1(2):101–10. doi:10.1007/s40139-013-0012-0.
6. Codrici E, Enciu AM, Popescu ID, Mihai S, Tanase C. Glioma stem cells and their microenvironments: providers of challenging therapeutic targets. *Stem Cells Int*. 2016;2016:5728438. doi:10.1155/2016/5728438.
7. Gilbertson RJ, Rich JN. Making a tumour's bed: glioblastoma stem cells and the vascular niche. *Nat Rev Cancer*. 2007;7(10):733–6. doi:10.1038/nrc2246.
8. Bao S, Wu Q, McLendon RE, Hao Y, Shi Q, Hjelmeland AB, Dewhirst MW, Bigner DD, Rich JN. Glioma stem cells promote radioresistance by preferential activation of the DNA damage response. *Nature*. 2006;444(7120):756–60. doi:10.1038/nature05236.
9. Hambardzumyan D, Bergers G. Glioblastoma: defining tumor niches. *Trends Cancer*. 2015;1(4):252–65. doi:10.1016/j.trecan.2015.10.009.
10. Eramo A, Ricci-Vitiani L, Zeuner A, Pallini R, Lotti F, Sette G, Pilozzi E, Larocca LM, Peschle C, De Maria R. Chemotherapy resistance of glioblastoma stem cells. *Cell Death Differ*. 2006;13(7):1238–41. doi:10.1038/sj.cdd.4401872.
11. Fidoamore A, Cristiano L, Antonosante A, d'Angelo M, Di Giacomo E, Astarita C, Giordano A, Ippoliti R, Benedetti E, Cimini A. Glioblastoma stem cells microenvironment: the paracrine roles of the niche in drug and radioresistance. *Stem Cells Int*. 2016;2016:6809105. doi:10.1155/2016/6809105.
12. Niibori-Nambu A, Midorikawa U, Mizuguchi S, Hide T, Nagai M, Komohara Y, Nagayama M, Hirayama M, Kobayashi D, Tsubota N, Takezaki T, Makino K, Nakamura H, Takeya M, Kuratsu J, Araki N. Glioma initiating cells form a differentiation niche via the induction of extracellular matrices and integrin alphaV. *PLoS ONE*. 2013;8(5):e59558. doi:10.1371/journal.pone.0059558.

13. Borovski T, De Sousa EMF, Vermeulen L, Medema JP. Cancer stem cell niche: the place to be. *Cancer Res.* 2011;71(3):634–9. doi:10.1158/0008-5472.CAN-10-3220.
14. Calabrese C, Poppleton H, Kocak M, Hogg TL, Fuller C, Hamner B, Oh EY, Gaber MW, Finklestein D, Allen M, Frank A, Bayazitov IT, Zakharenko SS, Gajjar A, Davidoff A, Gilbertson RJ. A perivascular niche for brain tumor stem cells. *Cancer Cell.* 2007;11(1):69–82. doi:10.1016/j.ccr.2006.11.020.
15. Hira VV, Ploegmakers KJ, Grevers F, Verbovsek U, Silvestre-Roig C, Aronica E, Tigchelaar W, Turnsek TL, Molenaar RJ, van Noorden CJF. CD133+ and Nestin+ glioma stem-like cells reside around CD31+ arterioles in niches that express SDF-1alpha, CXCR4, osteopontin and Cathepsin K. *J Histochem Cytochem.* 2015;63(7):481–93. doi:10.1369/0022155415581689.
16. Hira VVV, Breznik B, Vittori M, Loncq de Jong A, Mlakar J, Oostra RJ, Khurshed M, Molenaar RJ, Lah T, van Noorden CJF. Similarities between stem cell niches in glioblastoma and bone marrow: rays of hope for novel treatment strategies. *J Histochem Cytochem.* 2020;68(1):33–57. doi:10.1369/0022155419878416.
17. Hira VVV, Wormer JR, Kakar H, Breznik B, van der Swaan B, Hulsbos R, Tigchelaar W, Tonar Z, Khurshed M, Molenaar RJ, van Noorden CJF. Periarteriolar glioblastoma stem cell niches express bone marrow hematopoietic stem cell niche proteins. *J Histochem Cytochem.* 2018;66(3):155–73. doi:10.1369/0022155417749174.
18. Hira VVV, Aderetti DA, van Noorden CJF. Glioma stem cell niches in human glioblastoma are periarteriolar. *J Histochem Cytochem.* 2018;66(5):349–58. doi:10.1369/0022155417752676.
19. Zagzag D, Esencay M, Mendez O, Yee H, Smirnova I, Huang Y, Chiriboga L, Lukyanov E, Liu M, Newcomb EW. Hypoxia- and vascular endothelial growth factor-induced stromal cell-derived factor-1alpha/CXCR4 expression in glioblastomas: one plausible explanation of Scherer's structures. *Am J Pathol.* 2008;173(2):545–60. doi:10.2353/ajpath.2008.071197.
20. Zagzag D, Lukyanov Y, Lan L, Ali MA, Esencay M, Mendez O, Yee H, Voura EB, Newcomb EW. Hypoxia-inducible factor 1 and VEGF upregulate CXCR4 in glioblastoma: implications for angiogenesis and glioma cell invasion. *Lab Invest.* 2006;86(12):1221–32. doi:10.1038/labinvest.3700482.
21. Ohnishi S, Maehara O, Nakagawa K, Kameya A, Otaki K, Fujita H, Higashi R, Takagi K, Asaka M, Sakamoto N, Kobayashi M, Takeda H. Hypoxia-inducible factors activate CD133 promoter through ETS family transcription factors. *PLoS ONE.* 2013;8(6):e66255. doi:10.1371/journal.pone.0066255.
22. Soeda A, Park M, Lee D, Mintz A, Androutsellis-Theotokis A, McKay RD, Engh J, Iwama T, Kunisada T, Kassam AB, Pollack IF, Park DM. Hypoxia promotes expansion of the CD133-positive glioma stem cells through activation of HIF-1alpha. *Oncogene.* 2009;28(45):3949–59. doi:10.1038/onc.2009.252.
23. Seidel S, Garvalov BK, Wirta V, von Stechow L, Schanzer A, Meletis K, Wolter M, Sommerlad D, Henze A-T, Nistér M, Reifemberger G, Lundeberg J, Frisén J, Acker T. A hypoxic niche regulates glioblastoma stem cells through hypoxia inducible factor 2 alpha. *Brain.* 2010;133(Pt 4):983–95. doi:10.1093/brain/awq042.
24. Heddlestone JM, Li Z, Lathia JD, Bao S, Hjelmeland AB, Rich JN. Hypoxia inducible factors in cancer stem cells. *Br J Cancer.* 2010;102(5):789–95. doi:10.1038/sj.bjc.6605551.
25. Heddlestone JM, Li Z, McLendon RE, Hjelmeland AB, Rich JN. The hypoxic microenvironment maintains glioblastoma stem cells and promotes reprogramming towards a cancer stem cell phenotype. *Cell Cycle.* 2009;8(20):3274–84. doi:10.4161/cc.8.20.9701.
26. Goffart N, Kroonen J, Di Valentin E, Dedobbeleer M, Denne A, Martinive P, Rogister B. Adult mouse subventricular zones stimulate glioblastoma stem cells specific invasion through CXCL12/CXCR4 signaling. *Neuro Oncol.* 2015;17(1):81–94. doi:10.1093/neuonc/nou144.
27. Goffart N, Lombard A, Lallemand F, Kroonen J, Nassen J, Di Valentin E, Berendsen S, Dedobbeleer M, Willems E, Robe P, Bours V, Martin D, Martinive P, Maquet P, Rogister B. CXCL12 mediates glioblastoma resistance to radiotherapy in the subventricular zone. *Neuro Oncol.* 2017;19(1):66–77. doi:10.1093/neuonc/now136.
28. Altmann C, Keller S, Schmidt MHH. The role of SVZ stem cells in glioblastoma. *Cancers (Basel).* 2019;11(4):448. doi:10.3390/cancers11040448.
29. Jafri NF, Clarke JL, Weinberg V, Barani IJ, Cha S. Relationship of glioblastoma multiforme to the subventricular zone is associated with survival. *Neuro Oncol.* 2013;15(1):91–6. doi:10.1093/neuonc/nos268.
30. Adeberg S, Bostel T, König L, Welzel T, Debus J, Combs SE. A comparison of long-term survivors and short-term survivors with glioblastoma, subventricular zone involvement: a predictive factor for survival? *Radiat Oncol.* 2014;9:95. doi:10.1186/1748-717X-9-95.
31. Adeberg S, König L, Bostel T, Harrabi S, Welzel T, Debus J, Combs SE. Glioblastoma recurrence patterns after radiation therapy with regard to the subventricular zone. *Int J Radiat Oncol Biol Phys.* 2014;90(4):886–93. doi:10.1016/j.ijrobp.2014.07.027.
32. Wen B, Fu F, Hu L, Cai Q, Xie J. Subventricular zone predicts high velocity of tumor expansion and poor clinical outcome in patients with low grade astrocytoma. *Clin Neurol Neurosurg.* 2018;168:12–7. doi:10.1016/j.clineuro.2018.02.036.
33. Weinberg BD, Boreta L, Braunstein S, Cha S. Location of subventricular zone recurrence and its radiation dose predicts survival in patients with glioblastoma. *J Neurooncol.* 2018;138(3):549–56. doi:10.1007/s11060-018-2822-8.
34. Mistry AM, Dewan MC, White-Dzuro GA, Brinson PR, Weaver KD, Thompson RC, Ihrie RA, Chambless LB. Decreased survival in glioblastomas is specific to contact with the ventricular-subventricular zone, not subgranular zone or corpus callosum. *J Neurooncol.* 2017; 132(2):341–9. doi:10.1007/s11060-017-2374-3.

35. Mistry AM, Hale AT, Chambless LB, Weaver KD, Thompson RC, Ihrle RA. Influence of glioblastoma contact with the lateral ventricle on survival: a meta-analysis. *J Neurooncol*. 2017;131(1):125–33. doi:10.1007/s11060-016-2278-7.
36. van Dijken BRJ, Yan JL, Boonzaier NR, Li C, van Laar PJ, van der Hoorn A, van der Hoorn A, Price SJ. Subventricular zone involvement characterized by diffusion tensor imaging in glioblastoma. *World Neurosurg*. 2017;105:697–701. doi:10.1016/j.wneu.2017.06.075.
37. Mistry AM, Mummareddy N, Salwi S, Davis LT, Ihrle RA. Glioblastoma distance from the subventricular neural stem cell niche does not correlate with survival. *Front Oncol*. 2020;10:564889. doi:10.3389/fonc.2020.564889.
38. Chen L, Chaichana KL, Kleinberg L, Ye X, Quinones-Hinojosa A, Redmond K. Glioblastoma recurrence patterns near neural stem cell regions. *Radiother Oncol*. 2015;116(2):294–300. doi:10.1016/j.radonc.2015.07.032.
39. Reynolds BA, Weiss S. Generation of neurons and astrocytes from isolated cells of the adult mammalian central nervous system. *Science*. 1992;255(5052):1707–10. doi:10.1126/science.1553558.
40. Reynolds BA, Weiss S. Clonal and population analyses demonstrate that an EGF-responsive mammalian embryonic CNS precursor is a stem cell. *Dev Biol*. 1996;175(1):1–13. doi:10.1006/dbio.1996.0090.
41. Sanai N, Tramontin AD, Quinones-Hinojosa A, Barbaro NM, Gupta N, Kunwar S, Lawton MT, McDermott MW, Parsa AT, Verdugo JM-G, Berger MS, Alvarez-Buylla A. Unique astrocyte ribbon in adult human brain contains neural stem cells but lacks chain migration. *Nature*. 2004;427(6976):740–4. doi:10.1038/nature02301.
42. Quinones-Hinojosa A, Sanai N, Soriano-Navarro M, Gonzalez-Perez O, Mirzadeh Z, Gil-Perotin S, Romero-Rodriguez R, Berger MS, Garcia-Verdugo JM, Alvarez-Buylla A. Cellular composition and cytoarchitecture of the adult human subventricular zone: a niche of neural stem cells. *J Comp Neurol*. 2006;494(3):415–34. doi:10.1002/cne.20798.
43. Chojnacki AK, Mak GK, Weiss S. Identity crisis for adult periventricular neural stem cells: subventricular zone astrocytes, ependymal cells or both? *Nat Rev Neurosci*. 2009;10(2):153–63. doi:10.1038/nrn2571.
44. Coulter CL, Young IR, Browne CA, McMillen IC. Different roles for the pituitary and adrenal cortex in the control of enkephalin peptide localization and cortico-medullary interaction in the sheep adrenal during development. *Neuroendocrinology*. 1991;53(3):281–6. doi:10.1159/000125730.
45. Kokovay E, Goderie S, Wang Y, Lotz S, Lin G, Sun Y, Roysam B, Shen Q, Temple S. Adult SVZ lineage cells home to and leave the vascular niche via differential responses to SDF1/CXCR4 signaling. *Cell Stem Cell*. 2010;7(2):163–73. doi:10.1016/j.stem.2010.05.019.
46. Thomas RP, Nagpal S, Iv M, Soltys SG, Bertrand S, Pelpola JS, Ball R, Yang J, Sundaram V, Lavezo J, Born D, Vogel H, Brown JM, Recht LD. Macrophage exclusion after radiation therapy (MERT): a first in human phase I/II trial using a CXCR4 inhibitor in glioblastoma. *Clin Cancer Res*. 2019;25(23):6948–57. doi:10.1158/1078-0432.CCR.
47. Giordano FA, Link B, Glas M, Herrlinger U, Wenz F, Umansky V, Martin Brown J, Herskind C. Targeting the post-irradiation tumor microenvironment in glioblastoma via inhibition of CXCL12. *Cancers (Basel)*. 2019;11(3):272. doi:10.3390/cancers11030272.
48. Rabenstein M, Hucklenbroich J, Willuweit A, Ladwig A, Fink GR, Schroeter M, Langen K-J, Rueger MA. Osteopontin mediates survival, proliferation and migration of neural stem cells through the chemokine receptor CXCR4. *Stem Cell Res Ther*. 2015;6:99. doi:10.1186/s13287-015.
49. Deboux C, Ladraa S, Cazaubon S, Ghribi-Mallah S, Weiss N, Chaverot N, Ghribi-Mallah S, Weiss N, Chaverot N, Couraud PO, Baron-Van Evercooren A. Overexpression of CD44 in neural precursor cells improves trans-endothelial migration and facilitates their invasion of perivascular tissues in vivo. *PLoS ONE*. 2013;8(2):e57430. doi:10.1371/journal.pone.0057430.
50. Sawada R, Nakano-Doi A, Matsuyama T, Nakagomi N, Nakagomi T. CD44 expression in stem cells and niche microglia/macrophages following ischemic stroke. *Stem Cell Investig*. 2020;7:4. doi:10.21037/sci.2020.02.02.
51. Singh SK, Hawkins C, Clarke ID, Squire JA, Bayani J, Hide T, Henkelman RM, Cusimano MD, Dirks PB. Identification of human brain tumour initiating cells. *Nature*. 2004;432(7015):396–401. doi:10.1038/nature03128.
52. Wu B, Sun C, Feng F, Ge M, Xia L. Do relevant markers of cancer stem cells CD133 and Nestin indicate a poor prognosis in glioma patients? A systematic review and meta-analysis. *J Exp Clin Cancer Res*. 2015;34:44. doi:10.1186/s13046-015-0163-4.
53. Song WS, Yang YP, Huang CS, Lu KH, Liu WH, Wu WW, Lee Y-Y, Lo W-L, Lee S-D, Chen Y-W, Huang P-I, Chen M-T. Sox2, a stemness gene, regulates tumor-initiating and drug-resistant properties in CD133-positive glioblastoma stem cells. *J Chin Med Assoc*. 2016;79(10):538–45. doi:10.1016/j.jcma.2016.03.010.
54. Zhang M, Song T, Yang L, Chen R, Wu L, Yang Z, Fang J. Nestin and CD133: valuable stem cell-specific markers for determining clinical outcome of glioma patients. *J Exp Clin Cancer Res*. 2008;27:85. doi:10.1186/1756-9966-27-85.
55. Lathia JD, Hitomi M, Gallagher J, Gadani SP, Adkins J, Vasanji A, Liu L, Eyley CE, Heddleston JM, Wu Q, Minhas S, Soeda A, Hoepfner DJ, Ravin R, McKay RDG, McLendon RE, Corbeil D, Chenn A, Hjelmeland AB, Park DM, Rich JN. Distribution of CD133 reveals glioma stem cells self-renew through symmetric and asymmetric cell divisions. *Cell Death Dis*. 2011;2:e200. doi:10.1038/cddis.2011.80.
56. Podergajs N, Motaln H, Rajcevic U, Verbovsek U, Korsic M, Obad N, Espedal H, Vittori M, Herold-Mende

- C, Miletic H, Bjerkvig R, Turnšek TL. Transmembrane protein CD9 is glioblastoma biomarker, relevant for maintenance of glioblastoma stem cells. *Oncotarget*. 2016;7(1):593–609. doi:10.18632/oncotarget.5477.
57. Kolosa K, Motaln H, Herold-Mende C, Korsic M, Lah TT. Paracrine effects of mesenchymal stem cells induce senescence and differentiation of glioblastoma stem-like cells. *Cell Transplant*. 2015;24(4):631–44. doi:10.3727/096368915X687787.
58. Torsvik A, Rosland GV, Svendsen A, Molven A, Immervoll H, McCormack E, Lønning PE, Primon M, Sobala E, Tonn J-C, Goldbrunner R, Schichor C, Mysliwicz J, Lah TT, Motaln H, Knappskog S, Bjerkvig R. Spontaneous malignant transformation of human mesenchymal stem cells reflects cross-contamination: putting the research field on track—letter. *Cancer Res*. 2010;70(15):6393–6. doi:10.1158/0008-5472.CAN-10-1305.
59. Hira VVV, de Jong AL, Ferro K, Khurshed M, Molenaar RJ, van Noorden CJF. Comparison of different methodologies and cryostat versus paraffin sections for chromogenic immunohistochemistry. *Acta Histochem*. 2019;121(2):125–34. doi:10.1016/j.acthis.2018.10.011.
60. Chieco P, Jonker A, De Boer BA, Ruijter JM, van Noorden CJ. Image cytometry: protocols for 2D and 3D quantification in microscopic images. *Prog Histochem Cytochem*. 2013;47(4):211–333. doi:10.1016/j.proghi.2012.09.001.
61. Augé E, Bechmann I, Llor N, Vilaplana J, Krueger M, Pelegrí C. Corpora amylacea in human hippocampal brain tissue are intracellular bodies that exhibit a homogeneous distribution of neo-epitopes. *Sci Rep*. 2019;9(1):2063. doi:10.1038/s41598-018-38010-7.
62. Kierszenbaum AL. *Histology and cell biology. An introduction to pathology*. St. Louis, MI: Mosby; 2002.
63. Capela A, Temple S. LeX/ssea-1 is expressed by adult mouse CNS stem cells, identifying them as nonependymal. *Neuron*. 2002;35(5):865–75. doi:10.1016/s0896-6273(02)00835-8.
64. Corti S, Nizzardo M, Nardini M, Donadoni C, Locatelli F, Papadimitriou D, Salani S, Del Bo R, Ghezzi S, Strazzer S, Bresolin N, Comi GP. Isolation and characterization of murine neural stem/progenitor cells based on Prominin-1 expression. *Exp Neurol*. 2007;205(2):547–62. doi:10.1016/j.expneurol.2007.03.021.
65. Gil-Perotin S, Marin-Husstege M, Li J, Soriano-Navarro M, Zindy F, Roussel MF, Garcia-Verdugo J-M, Casaccia-Bonnel P. Loss of p53 induces changes in the behavior of subventricular zone cells: implication for the genesis of glial tumors. *J Neurosci*. 2006;26(4):1107–16. doi:10.1523/JNEUROSCI.3970-05.2006.
66. Liu X, Bolteus AJ, Balkin DM, Henschel O, Bordey A. GFAP-expressing cells in the postnatal subventricular zone display a unique glial phenotype intermediate between radial glia and astrocytes. *Glia*. 2006;54(5):394–410. doi:10.1002/glia.20392.
67. Ho SY, Ling TY, Lin HY, Liou JT, Liu FC, Chen IC, Lee S-W, Hsu Y, Lai D-M, Liou H-H. SDF-1/CXCR4 signaling maintains stemness signature in mouse neural stem/progenitor cells. *Stem Cells Int*. 2017;2017:2493752. doi:10.1155/2017/2493752.
68. Qin EY, Cooper DD, Abbott KL, Lennon J, Nagaraja S, Mackay A, Jones C, Vogel H, Jackson PK, Monje M. Neural precursor-derived pleiotrophin mediates subventricular zone invasion by glioma. *Cell*. 2017;170(5):845–59.e19. doi:10.1016/j.cell.2017.07.016.
69. Morshead CM, van der Kooy D. Disguising adult neural stem cells. *Curr Opin Neurobiol*. 2004;14(1):125–31. doi:10.1016/j.conb.2004.01.008.
70. Doetsch F, Caille I, Lim DA, Garcia-Verdugo JM, Alvarez-Buylla A. Subventricular zone astrocytes are neural stem cells in the adult mammalian brain. *Cell*. 1999;97(6):703–16. doi:10.1016/s0092-8674(00)80783-7.
71. Casper KB, McCarthy KD. GFAP-positive progenitor cells produce neurons and oligodendrocytes throughout the CNS. *Mol Cell Neurosci*. 2006;31(4):676–84. doi:10.1016/j.mcn.2005.12.006.
72. Liu H, Sun Y, O'Brien JA, Franco-Barraza J, Qi X, Yuan H, Jin W, Zhang J, Gu C, Zhao Z, Yu C, Feng S, Yu X. Necroptotic astrocytes contribute to maintaining stemness of disseminated medulloblastoma through CCL2 secretion. *Neuro Oncol*. 2020;22:625–38. doi:10.1093/neuonc/noz214.
73. Thapa R, Wilson GD. The importance of CD44 as a stem cell biomarker and therapeutic target in cancer. *Stem Cells Int*. 2016;2016:2087204. doi:10.1155/2016/2087204.
74. Trautmann F, Cojoc M, Kurth I, Melin N, Bouchez LC, Dubrovskaya A, Peitzsch C. CXCR4 as biomarker for radioresistant cancer stem cells. *Int J Radiat Biol*. 2014;90(8):687–99. doi:10.3109/09553002.2014.906766.
75. Suva ML, Tirosh I. The glioma stem cell model in the era of single-cell genomics. *Cancer Cell*. 2020;37(5):630–6. doi:10.1016/j.ccell.2020.04.001.
76. Brown DV, Daniel PM, D'Abaco GM, Gogos A, Ng W, Morokoff AP, Mantamadiotis T. Coexpression analysis of CD133 and CD44 identifies proneural and mesenchymal subtypes of glioblastoma multiforme. *Oncotarget*. 2015;6(8):6267–80. doi:10.18632/oncotarget.3365.
77. Mooney KL, Choy W, Sidhu S, Pelargos P, Bui TT, Voth B, Barnette N, Yang I. The role of CD44 in glioblastoma multiforme. *J Clin Neurosci*. 2016;34:1–5. doi:10.1016/j.jocn.2016.05.012.
78. Akita M, Tanaka K, Matsumoto S, Komatsu K, Fujita K. Detection of the hematopoietic stem and progenitor cell marker CD133 during angiogenesis in three-dimensional collagen gel culture. *Stem Cells Int*. 2013;2013:927403. doi:10.1155/2013/927403.
79. Hilbe W, Dirnhofer S, Oberwasserlechner F, Schmid T, Gunsilius E, Hilbe G, Wöll E, Kähler CM. CD133 positive endothelial progenitor cells contribute to the tumour vasculature in non-small cell lung cancer. *J Clin Pathol*. 2004;57(9):965–9. doi:10.1136/jcp.2004.016444.
80. Sekine A, Nishiwaki T, Nishimura R, Kawasaki T, Urushibara T, Suda R, Suzuki T, Takayanagi S, Terada J, Sakao S, Tada Y, Iwama A, Tatsumi K. Prominin-1/CD133 expression as potential tissue-resident vascular

- endothelial progenitor cells in the pulmonary circulation. *Am J Physiol Lung Cell Mol Physiol*. 2016;310(11):L1130–42. doi:10.1152/ajplung.00375.2014.
81. Hira VVV, Van Noorden CJF, Carraway HE, Maciejewski JP, Molenaar RJ. Novel therapeutic strategies to target leukemic cells that hijack compartmentalized continuous hematopoietic stem cell niches. *Biochim Biophys Acta Rev Cancer*. 2017;1868(1):183–98. doi:10.1016/j.bbcan.2017.03.010.
82. Lee JH, Lee JE, Kahng JY, Kim SH, Park JS, Yoon SJ, Um J-Y, Kim WK, Lee J-K, Park J, Kim EH, Lee J-H, Lee J-H, Chung W-S, Ju YS, Park S-H, Chang JH, Kang S-G, Lee JH. Human glioblastoma arises from subventricular zone cells with low-level driver mutations. *Nature*. 2018;560(7717):243–7. doi:10.1038/s41586-018-0389-3.
83. Sanai N, Alvarez-Buylla A, Berger MS. Neural stem cells and the origin of gliomas. *N Engl J Med*. 2005;353(8):811–22. doi:10.1056/NEJMra043666.